

Investigation of impact of different working fluids on the operational characteristics of miniature LHP with flat evaporator

Zhichun Liu, Dongxing Gai, Huan Li, Wei Liu*, Jinguo Yang, Mengmeng Liu

School of Energy and Power Engineering, Huazhong University of Science and Technology, Wuhan 430074, China

ARTICLE INFO

Article history:

Received 29 September 2010

Accepted 15 June 2011

Available online 23 June 2011

Keywords:

LHP

Working fluid

Temperature oscillations

ABSTRACT

Experimental studies are carried out on the operational characteristic of LHP with a flat evaporator, the difference between methanol and acetone as working fluid is especially investigated in the study. Result shows that the flat-plate LHP has a good startup characteristic and ability to adapt heat load change. Compared with LHP-methanol, the LHP-acetone starts up faster, and when it comes to steady status, the temperature of evaporator wall is lower; however, heat transfer limitation of LHP-acetone is far less than that of LHP-methanol.

Crown Copyright © 2011 Published by Elsevier Ltd. All rights reserved.

1. Introduction

Loop heat pipes (LHPs) are high efficiency heat transfer devices, which utilize phase changing of working fluid to transfer heat and capillary force to drive fluid cycle. The main components of an LHP include an evaporator, a condenser, a vapor line and liquid line. LHP can be seen as an improved version of a heat pipe that solve limitations of the conventional heat pipe by completely separating the liquid and vapor phases from each other by separated lines and localizing the capillary structure in the evaporator only. As a result, LHPs possess all the main advantages of conventional heat pipes, but owing to the original design and special properties of the capillary structure, they are capable of transferring heat load for distances up to several meters at any orientation in the gravity field, or to several tens of meters in a horizontal position [1]. Their good heat transfer performance have been traditionally utilized to address the thermal control problem in spacecraft, and successfully applied in many space tasks. Recently, the applications of LHPs have been extended to terrestrial surroundings such as electronic cooling systems.

LHP is first invented in the former Soviet Union in 1974 [2]. Many studies [3–7] have been carried out to improve the reliability and performance of LHP. Li et al. [8] conduct an experimental study on LHP with square flat evaporator, and their result shows that LHP can transfer heat load of more than 600 W (with a heat flux in excess of $100\text{W}/\text{cm}^2$) with no dryout in evaporator, and in their paper, they propose two startup modes, boiling trigger

startup and evaporation trigger startup, to explain the varying startup behavior for different heat load. Singh et al. [5] conduct an experimental investigation for thermal characteristics of a miniature loop heat pipe with a flat evaporator, and they find that LHP is able to startup at input power as low as 5 W, but the startup time is very long; At the horizontal orientation, LHP can transfer maximum heat load of 70 W with evaporator temperature below $100 \pm 5^\circ\text{C}$, and the thermal resistance of LHP lies between 0.17 and $5.66^\circ\text{C}/\text{W}$. Vershinin et al. [9] study the hysteresis phenomena in LHP, they find that temperature hysteresis is connected with changes in the liquid distribution between the compensation chamber and the condenser, and they distinguish three types of temperature hysteresis according to their analysis for different temperature hysteresis phenomena. Tang et al. [10] develop a novel sintered-grooved composite wick structures, and they identify and locate the liquid meniscus by infrared thermal imaging, with ethanol as working fluid. In their investigation, they find that the capillary force of composite wick is larger than that of grooved and sintered ones. Lin et al. [11] perform a fundamental study of a dual compensation chamber loop heat pipe (DCCLHP) through partial visualization of the flow phenomenon inside its compensation chambers and the condenser. Both startup and steady state performance of the DCCLHP and the influence of initial vapor–liquid distribution, startup heat load, heat sink temperature and relative orientations on the performance of the DCCLHP are studied. Wang et al. [12] fabricate a micro loop heat pipe using MEMS technology, and the issue of depriming in a miniature capillary pump loop (MCPL) is effectively controlled, the endurance of MCPL for the depriming problem can be executed by yielding input heat flux of $185.2\text{ W}/\text{cm}^2$ at an evaporator

* Corresponding author. Tel.: +86 27 8754 2618.

E-mail address: w_liu@hust.edu.cn (W. Liu).

temperature of 165 °C, thus revealing that this model provides excellent cooling performance.

The main object of the present study is to investigate the impact of different working fluids on the operational characteristics of miniature flat-plate LHP, and other parameters, such as tilt angle and charging ratio, are also considered in the experiment.

2. Flat-plate LHP experimental system

The experimental system in the present study consists of four subsystems: LHP system, heating system, ambience temperature control system, and data acquisition system. Fig. 1 shows the flat-plate LHP system, which is composed by an evaporator, an air-cooled fin-and-tube type condenser, a vapor line and a liquid line. The wick in evaporator is 4 mm thickness, which is made up of 82 layers 500 grids stainless steel mesh. The evaporator, condenser and vapor/liquid lines are all made of pure copper. The geometric characteristics of the LHP are shown in Table 1. For charging, the loop is firstly evacuated to 3.0×10^{-4} Pa and then filled with methanol (99.5% purity), after performance test of LHP, the loop is then evacuated to 3.0×10^{-4} Pa again and filled with acetone (99.5% purity). Twelve T-type thermocouples with ± 0.2 °C accuracy, which are calibrated by temperature calibrator, are used to measure temperature at different locations of the LHP and the ambient air. The heat load is tested by wattmeter, whose relative test accuracy is 0.025%. Fig. 1 also shows the placement of the thermocouples on the LHP system. All the instruments are connected to the Keithley-2700 data acquisition system which helps to monitor and record test data from the LHP prototype. In order to test the thermal performance of the LHP, a heat load simulator in the form of copper block with two embedded cartridge heater and active area of 40×30 mm is used. For the purpose of minimizing heat loss to the ambient, the heat load simulator is thermally insulated using 10 mm thickness nano-adiabatic material with conductivity of 0.012 W/m K. The temperatures of two sides of the heat insulation material are measured during the experiment, and the heat loss at different heat load can be calculated. According to the calculation, the heat loss is less than 0.3% of total power applied to the simulator.

3. Results and discussion

3.1. Thermal resistance analyze

According to theory of LHP [13], define thermal resistance of LHP as follow:

$$R_{LHP} = (T_{evap} - T_{cond}) / Q$$

Where T_{evap} is the mean temperature of evaporator active heated zone; T_{cond} is the average temperature of condenser; Q is the applied heat load. Hereinafter, R_{LHP} -methanol means the R_{LHP} of LHP with methanol as working fluid, and R_{LHP} -acetone means the R_{LHP} of LHP with acetone as working fluid. And for convenience, LHP-methanol stands for LHP system with methanol as working fluid, and LHP-acetone stands for LHP system with acetone as working fluid.

Define charging ratio as:

$$\alpha = V_l / V_{total} \times 100\%$$

Where, V_l is the volume of working fluid charged at ambient temperature of 20 °C, and V_{total} is the cavity volume of the whole loop, including condenser, connecting line, grooves, compensation chamber (CC), and gaps in the wick.

From Fig. 2, it can be seen that R_{LHP} declines as heat load increases. At the same operation condition, the R_{LHP} -acetone is lower, the reason for this is that, at the atmospheric pressure, the boiling point of acetone (56.6 °C) is lower than that of methanol (64.7 °C), and evaporation of acetone can take place at a lower temperature, leading to a lower T_{evap} . When $\alpha = 50\%$ or $\alpha = 60\%$ and heat load between 12 W and 60 W, R_{LHP} -methanol is 28.77% higher than that of R_{LHP} -acetone. From Fig. 2 it can be also obtained that, R_{LHP} -acetone is lowest at $\alpha = 60\%$, while R_{LHP} -methanol is lowest at $\alpha = 50\%$.

3.2. Characteristic of startup

When heat load is applied to the evaporator, part of the applied heat can be transferred to liquid core or compensation chamber, which is so called heat leak. For LHP with flat-plate evaporator, the

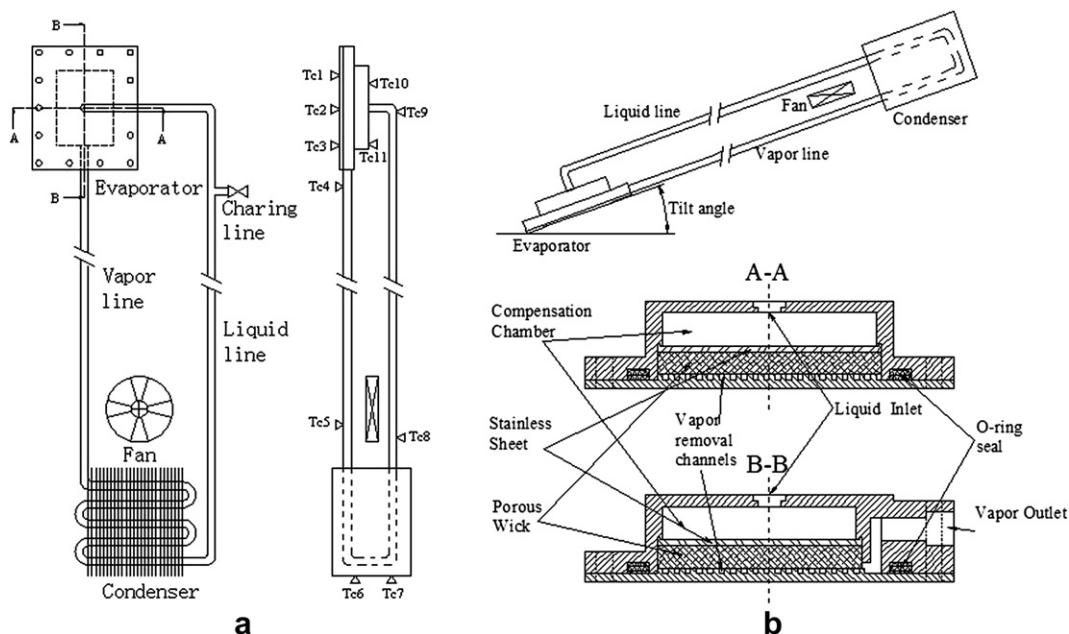


Fig. 1. Schematics of the LHP. (a) Top and side view of the LHP and the placement of the thermocouple points. (b) Cross section of the LHP evaporator.

Table 1
Geometric characteristics of the experimental LHP.

Evaporator	
Active heated zone	
Thickness (mm)	1.5
Length/width (mm)	40/30
Groove thickness (mm)	1
Fin number	18 × 15
Fin width (mm)	1 × 1
Wall	
Thickness (mm)	1.5
Porous sheet	
Thickness (mm)	0.5
Compensation chamber	
Length/width (mm)	34.5/30
Height (mm)	6
Porous wick	
Length/width/thickness (mm)	36.5/30/4
Material	316L
Parameter of mesh	500#, 82 layers
Vapor line	
Diameter (O/I)(mm)	6/4
Length (mm)	320
Liquid line	
Diameter (O/I)(mm)	6/4
Length (mm)	530
Condenser	
Diameter (O/I)(mm)	6/4
Length (mm)	810
Fin thickness (mm)	0.05
Fin length/width (mm)	100/20
Fan rotate speed (rpm)	3000

heat leak problem is more serious than that of LHP with cylindrical evaporator, since the former is easier to transfer more heat from the heating wall to compensation chamber (CC) than the later. The degree of subcooling is the temperature difference of saturated vapor in compensation chamber and the returning liquid. With higher degree of subcooling, compensation chamber can tolerate more heat conducted from heating wall, which reduces the possibility of evaporating of liquid in the compensation chamber. If the transferred heat is larger enough to reduce the subcooling of the returning fluid, bubbles will generate in the CC, which can decrease cycling quantity or block working fluid flow back to CC, or even lead to dryout in the wick. The back conduction in the flat-plate evaporator has a great impact on operation of the LHP, especially on the

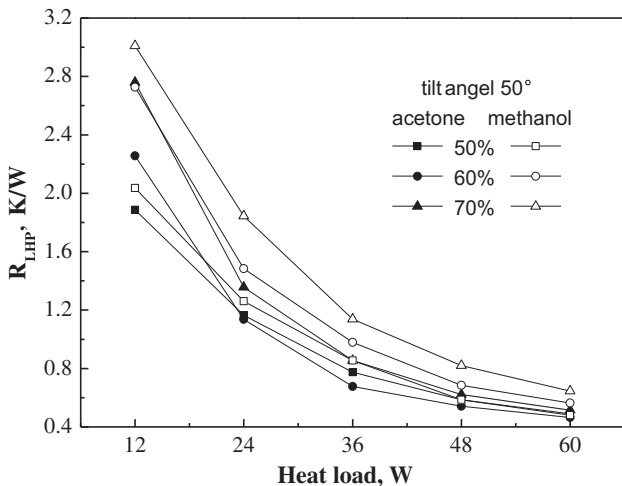


Fig. 2. R_{LHP} at different charging ratio.

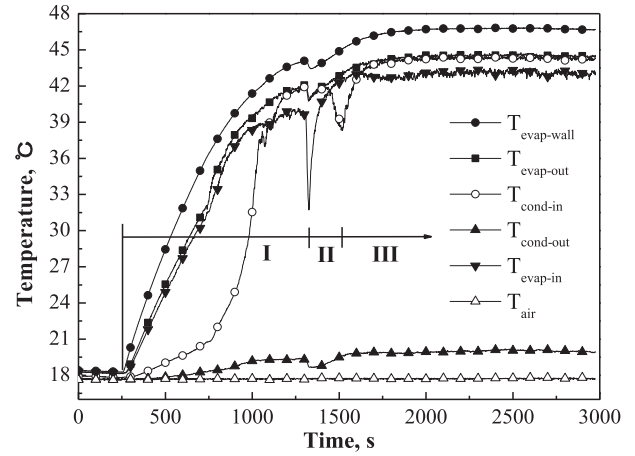


Fig. 3. 10°-60 vol.%-12 W (acetone) startup ($\Delta T_{sub}=1.5$ °C).

startup process. Therefore it is one of key characteristics of LHP that whether LHP can startup successfully [14–17]. The experimental results of performance tests for LHP under different charging ratios, tilt angles, heat loads and degree of subcooling can be found in Figs. 3–8. In the study, at heat loads range of 12–60 W (12 W as an interval), startup experiment is carried out with two kinds of working fluids: methanol and acetone, at three different tilt angles (10°, 50°, 90°), and at three different charging ratios (50 vol.%, 60 vol.%, 70 vol.%), and result shows that the flat-plate LHP can startup successfully without dryout, which means the LHP have a good startup characteristic.

The startup of loop heat pipe consists of three main processes: (I) clear off the liquid from evaporator grooves, vapor line and part of condenser, the I-zone is the first part of the startup time; (II) generate enough pressure difference across the porous wick which is necessary to drive the working fluid around the loop, the II-zone is the second part of the startup time; and (III) LHP achieves the final running state. When LHP starts up successfully, it can present two kinds of running states: (I) Steady state, that is, temperature of every component keeps constant. (II) Temperature oscillation state, that is, the temperature of every component keeps oscillating with different amplitudes and the same frequencies [18,19].

With larger tilt angle, the gravity provides more driven force for subcooled liquid returning to the evaporator, correspondingly, the

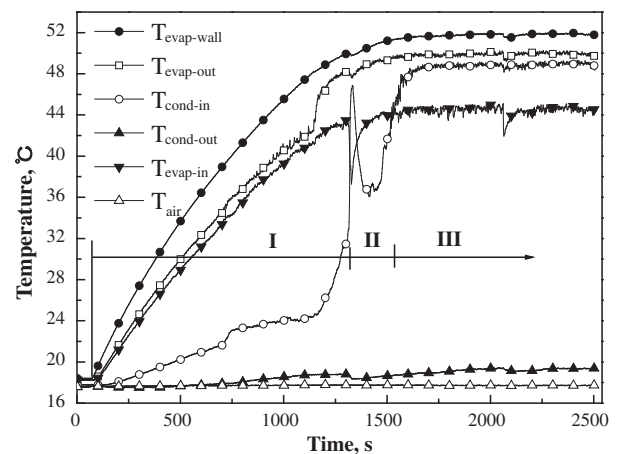


Fig. 4. 10°-60 vol.%-12 W (methanol) startup ($\Delta T_{sub}=14$ °C).

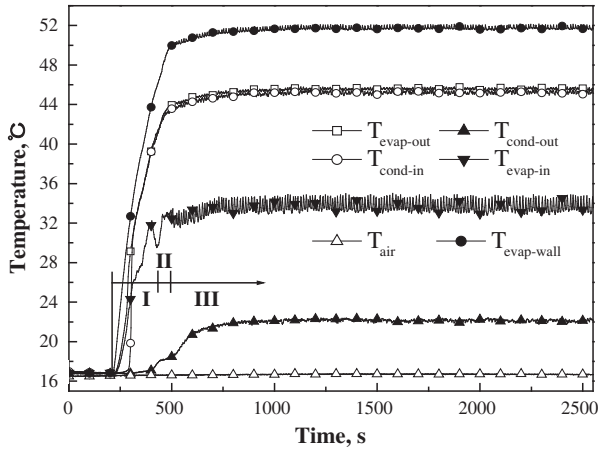


Fig. 5. 50°-50 vol.-%-60 W (acetone) startup ($\Delta T_{sub}=10\text{ }^{\circ}\text{C}$).

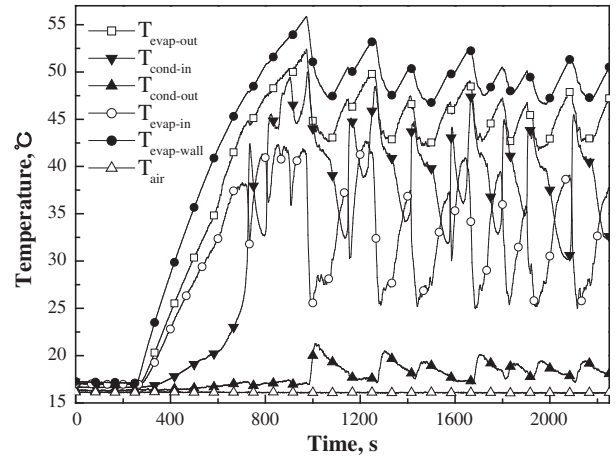


Fig. 7. 90°-70 vol.-%-24 W (acetone) startup ($\Delta T_{sub}=10\text{ }^{\circ}\text{C}$).

capillary pressure will reduce if other operation conditions keep the same. The vaporization point of working fluid depends on the pressure inside the LHP. So if the tilt angle become larger, the capillary pressure drops in the LHP, the vaporization point of fluid drops too, as a result, the temperature of evaporator wall decreases. With respect to charging ratio, the larger the ratio is, the less the space for liquid vaporizing, so the pressure inside the LHP increase, leading to a high temperature of evaporator wall.

From Figs. 3–6, it can be seen that, at the same working condition, LHP-methanol and LHP-acetone have similar startup phenomena. (I) When heat load increases, the startup time decreases, and correspondingly, the $T_{evap-wall}$ is higher. (II) The startup time of LHP-acetone is relatively shorter, after achieving steady state, $T_{evap-wall}$ is lower. (III) In the process of startup, there are some temperature oscillations at the inlet of evaporator, this is mainly because inlet is under the combined influence of back conduction and subcooled working fluid. For example, in Fig. 6, at the first half of I-zone, evaporator is heated up and no vapor is generated, $T_{evap-in}$ gets higher due to backward heat conduction. At second half of I-zone, vapor push working fluid into CC, then $T_{evap-in}$ plummets sharply because subcooled working liquid flow back into evaporator. At the first half of II-zone, the temperature of upper surface of wick keeps rising, forming vapor–liquid meniscus gradually. However, the wick cannot supply sufficient capillary force to circle the loop, $T_{evap-in}$ rises again under the influence of

backward heat conduction. At second half of II-zone, capillary force is eventually big enough to drive the loop circle, $T_{evap-in}$ again fall down due to the returning of the subcooled working fluid. III-zone is the final running state of the loop. (IV) At low heat load, the LHP-acetone starts up faster and $T_{evap-wall}$ is lower. However, the latent heat of vaporization of acetone ($5.2 \times 10^5\text{ J/kg}$) is less than half of methanol's ($1.12 \times 10^6\text{ J/kg}$), so at the same operation condition, the flow rate of LHP-acetone is more than twice of that of LHP-methanol, which leads to a higher hydraulic resistance. The surface tension of acetone is almost equally to that of methanol, therefore, heat transfer limitation of LHP-acetone is much smaller. In the experiments, LHP-acetone can dissipate 72 W, while LHP-methanol can achieve to 120 W.

3.3. Temperature oscillation

In the experiments, temperature oscillations are found in LHP system at different tilt angle and charging ratio, as shown in Table 2 and Table 3. The conducted investigations make it possible to classify three main types of the LHP operating temperature oscillations according to the amplitude and frequency [18]. The first type is characterized by a low-amplitude (no more than 1 °C) and a high-frequency; The second type is also characterized by a low-amplitude (no more than several centigrade degrees), but its

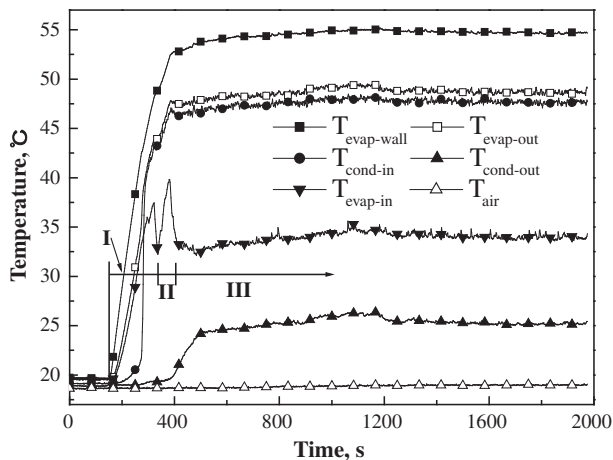


Fig. 6. 50°-50 vol.-%-60 W (methanol) startup ($\Delta T_{sub}=12\text{ }^{\circ}\text{C}$).

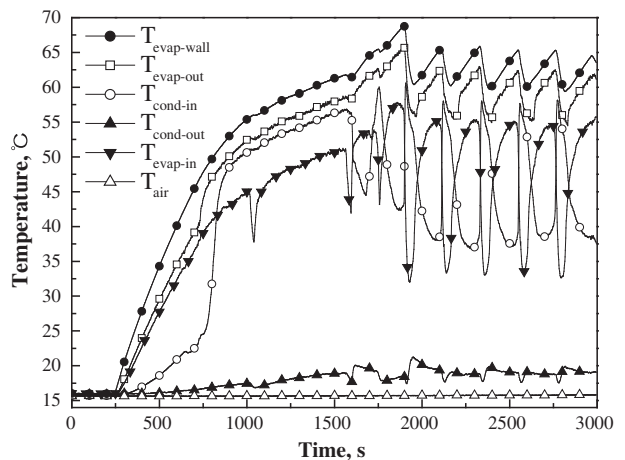


Fig. 8. 90°-70 vol.-%-24 W (methanol) startup ($\Delta T_{sub}=12\text{ }^{\circ}\text{C}$).

Table 2Amplitude and periods of the temperature oscillations of $T_{\text{evap-wall}}$ at different operation conditions (Methanol).

Operation condition (W)	Amplitude (°C)	Periods (s)
10°-50 vol.%	36	1.81
	48	2.42
	60	1.32
10°-70 vol.%	12	1.07
	24	12.54
50°-70 vol.%	12	7.82
	24	8.3
	36	11.1
50°,90°-50 vol.%	No obvious oscillation	
10°-60 vol.%	24	7.27
	36	8.46
50°-60 vol.%	24	3.73
	36	5.49
90°-60 vol.%	24	4.85
	36	1.34
90°-70 vol.%	24	6.32
	36	7.66

period is longer and reaches to several minutes; The third type is distinguished by high amplitude of temperature oscillation, which reaches to tens of centigrade degrees, and a still longer period, which may be equal to tens of minutes.

Figs. 7 and 8 show the startup of LHP-acetone and LHP-methanol under the same operation condition of 90°-70 vol.-%-24 W respectively. It can be seen from the figures that the temperatures of different components oscillate with different amplitude and the same frequency. The amplitude at evaporator inlet and condenser inlet is the highest, at evaporator wall and vapor line is the second, and at condenser wall and liquid line is the least. This is because there exists vapor/liquid two-phase region in CC and inlet of the condenser, whose complexity can lead to temperature oscillation. The temperature oscillations are very complicated, sometimes the oscillation is random and chaotic, as shown in Fig. 7, and the amplitude and frequency of temperature oscillation is irregular.

The temperature oscillations have undesirable effect on LHP operation. Taking LHP-methanol as an example, at 10°-70 vol.-%-24 W operation condition, the amplitude is as high as 12.5 °C, and $T_{\text{evap-wall}}$ reaches to 75 °C although heat load is still very low. Therefore, when LHP is applied to cool the device demanding high precision temperature control, heat load range leading to large temperature oscillation should be carefully avoided. Both changing tilt angle and charging ratio can minimize the temperature oscillation. Taking LHP-methanol as an example, at 10°-70 vol.-%-24 W

operation condition, amplitude is as high as 12.54 °C, while at 10°-50 vol.-%-24 W operation condition, the oscillations disappear. Changing working fluid also can minimize oscillation, at 10°-50 vol.-%-24 W working condition, the oscillations occur in LHP-methanol, while not exist in LHP-acetone.

Comparing Table 2 and Table 3, it can be seen that range of heat load causing temperature oscillations in LHP-acetone is mainly between 24 W and 36 W, and in LHP-methanol is between 12 W and 60 W, which indicates LHP-acetone has a larger oscillation heat load range than LHP-methanol. In the overall view, the amplitude of LHP-acetone is within 4 °C, 5.23 °C the maximum. With respect to the LHP-methanol, several amplitudes are larger than 7 °C, 12.54 °C the maximum. Therefore, LHP-methanol has fiercer oscillation than LHP-acetone. From Table 2 and Table 3, the LHP-methanol has a longer oscillation period, 520 s the maximum, while the period of LHP-acetone is within 120 s. In conclusion, compared with LHP-acetone, LHP-methanol has a larger oscillation heat load range and fiercer temperature oscillation.

Both LHP-methanol and LHP-acetone have few oscillation at $\alpha = 50\%$, especially at 50°-50 vol.-% and 90°-50 vol.-%. At $\alpha = 70\%$, both of them have large oscillation, and the fiercest oscillation occurs at 10°-70 vol.-%. Different working fluid can change range of heat load causing oscillation and the fierceness of oscillation, but it can't eliminate oscillation constitutionally. The oscillation is strongly related with charging ratio, tilt angle, property of working fluid, system structure and material. The occurrence of temperature oscillation depends on distribution of gas-liquid in the compensation chamber. When the distribution reaches to a critical status, the equilibrium breaks down and the oscillation happens. Usually, there is thermal energy equilibrium between flow thermal energy of returning liquid, back heat conduction, and heat dissipation with circumstance in evaporator. With the increasing of heat load, correspondingly, the heat leak will increase, and the mass flow rate will also increase, as the result, above mentioned equilibrium can remain stable. With the further increasing of the heat load, the thermal energy of returning liquid cannot compensate heat transfer of the back conduction, the temperature of compensation will increase to get a new equilibrium, and then the subcooled returning fluid flow rate will increase, due to the cooling effect, the temperature of the compensation chamber will decrease, as a result, the working temperate will also decrease. And this is critical status when LHP reaches this working status. When LHP comes to the critical status, the temperature of LHP can oscillate. In a large tilt angle condition, the amount of working liquid in the compensation chamber is relatively large, so a higher heat load is acquired for liquid to vaporize in compensation chamber to reach to the critical status and oscillate.

4. Conclusion

In the study, the operational characteristics of flat-plate LHP with different working fluids are investigated experimentally and several findings can be summarized as follows:

1. Compared with LHP-methanol, the LHP-acetone starts up faster, and when it comes to steady state, the temperature of evaporator wall is lower;
2. From the point of view of thermal resistance, $R_{\text{LHP-acetone}}$ is smaller than $R_{\text{LHP-methanol}}$ at the same operation condition;
3. At the same operation condition, the heat transfer limitation of LHP-acetone is far less than that of LHP-methanol;
4. Compared with LHP-acetone, there is larger heat load region inducing temperature oscillation and fiercer oscillation in LHP-methanol.

Table 3Amplitude and periods of the temperature oscillations of $T_{\text{evap-wall}}$ at different operation conditions (Acetone).

Operation condition (W)	Amplitude (°C)	Periods (s)
10°-50 vol.%	24	0.75
10°-70 vol.%	24	3.27
	36	5.23
50°-60 vol.%	24	2.92
	36	0.32
90°-60 vol.%	24	2.53
	36	0.72
10°-60 vol.%	36	1.74
50°,90°-50 vol.%	No obvious oscillation	
50°-70 vol.%	24	4.18
	36	1.03
90°-70 vol.%	24	4.01
	36	0.15

Acknowledgements

This research is supported by the National Natural Science Foundation of China (No. 50906026, No. 50876035).

References

- [1] Y.F. Maydanik, Loop heat pipes (review), *Applied Thermal Engineering* 25 (2005) 635–657.
- [2] Y. Gerasimov, Y.F. Maydanik, USSR Inventors Certificate 449213 (1974).
- [3] D.A. Wolf, D.M. Ernst, A.L. Phillips, Loop heat pipes—their performance and potential. SAE Paper No. 941575.
- [4] G.P. Celata, M. Cumo, M. Furrer, Experimental tests of a stainless steel loop heat pipe with flat evaporator, *Experimental Thermal and Fluid Science* 34 (7) (2010) 866–878.
- [5] R. Singh, A. Akbarzadeh, M. Mochizuki, Operational characteristics of a miniature loop heat pipe with flat evaporator, *International Journal of Thermal Sciences* 47 (11) (2008) 1504–1515.
- [6] G. Wang, D. Mishkinis, D. Nikanpour, Capillary heat loop technology: space applications and recent Canadian activities, *Applied Thermal Engineering* 28 (4) (2008) 284–303.
- [7] D.X. Gai, Z.C. Liu, W. Liu, J.G. Yang, Operational characteristics of a miniature loop heat pipe with flat evaporator, *Heat Mass Transfer* 46 (2009) 267–275.
- [8] J. Li, D.M. Wang, G.P. Peterson, Experimental studies on a high performance compact loop heat pipe with a square flat evaporator, *Applied Thermal Engineering* 30 (2010) 741–752.
- [9] S.V. Vershinin, Y.F. Maydanik, Hysteresis phenomena in loop heat pipes, *Applied Thermal Engineering* 27 (2007) 962–968.
- [10] Y. Tang, D.X. Deng, L.S. Lu, et al., Experimental investigation on capillary force of composite wick structure by IR thermal imaging camera, *Experimental Thermal and Fluid Science* 34 (2) (2010) 190–196.
- [11] G.P. Lin, N. Li, L.Z. Bai, et al., Experimental investigation of a dual compensation chamber loop heat pipe, *International Journal of Heat and Mass Transfer* 53 (15–16) (2010) 3231–3240.
- [12] C.T. Wang, T.S. Leu, T.M. Lai, Micro capillary pumped loop system for a cooling high power device, *Experimental Thermal and Fluid Science* 32 (5) (2008) 1090–1095.
- [13] R.R. Riehl, T. Dutra, Development of an experimental loop heat pipe for application in future space missions, *Applied Thermal Engineering* 25 (2005) 101–112.
- [14] W.H. Lee, K.H. Park, K.J. Lee, Study on Working Characteristics of Loop Heat Pipe Using a Sintered Metal Wick, in: 13th IHPC, 265–269 (2004) Shanghai, China.
- [15] H.X. Zhang, G.P. Lin, D. Ding, X.G. Shao, Experimental investigation for loop heat pipe startup, *Science in China, Series E* 35 (1) (2005) 17–30.
- [16] Y.M. Chen, M. Groll, R. Mertz, Steady-state and transient performance of a miniature loop heat pipe, *International Journal of Thermal Sciences* 45 (2006) 1084–1090.
- [17] L.Z. Bai, G.P. Ling, H.X. Zhang, Experimental investigation of steady operation for a gravity-assisted loop heat pipe, *Journal of Aerospace* 29 (5) (2008) 1112–1117.
- [18] S.V. Vershinin, Y.F. Maydanik, Investigation of pulsations of the operating temperature in a miniature loop heat pipe, *International Journal of Heat and Mass Transfer* 50 (2007) 5232–5240.
- [19] J. Ku, L. Ottenstein, M. Kobel, P. Rogers, T. Kaya, Temperature oscillations in loop heat pipe operation, *AIP Conference Proceedings* 552 (1) (2001) 255–262.

Nomenclature

- $T_{evap-wall}$: average temperature of evaporator wall, °C
 $T_{evap-in}$: temperature of evaporator inlet, °C
 $T_{evap-out}$: temperature of evaporator outlet, °C
 $T_{cond-in}$: temperature of condenser inlet, °C
 $T_{cond-out}$: temperature of condenser outlet, °C
 $T_{cond-fin}$: average temperature of fins in the last row, °C
 T_{air} : ambient temperature, °C
 ΔT_{sub} : degree of subcooling, °C
 Q : heat load, W
 α : charging ratio, %
 θ : tilt angle, °